Published in final edited form as:

Basic Res Cardiol. 2017 May ; 112(3): 33. doi:10.1007/s00395-017-0622-5.

IL-10 improves cardiac remodeling after myocardial infarction by stimulating M2 macrophage polarization and fibroblast activation

Mira Jung[1], **Yonggang Ma**[1], **Rugmani Padmanabhan Iyer**[1], **Kristine Y. DeLeon-Pennell**[1,4], **Andriy Yabluchiansky**[2], **Michael R. Garrett**[3], and **Merry L. Lindsey**[1,4]

[1]Department of Physiology and Biophysics, Mississippi Center for Heart Research, University of Mississippi Medical Center, 2500 North State St., Jackson, MS 39216-4505, USA

[2]Donald W. Reynolds Department of Geriatric Medicine, Reynolds Oklahoma Center on Aging, University of Oklahoma Health Sciences Center, Oklahoma City, USA

[3]Department of Pharmacology and Toxicology, UMMC, Jackson, MS, USA

[4]Research Service, G.V. (Sonny) Montgomery Veterans Affairs Medical Center, Jackson, MS, USA

Abstract

Inflammation resolution is important for scar formation following myocardial infarction (MI) and requires the coordinated actions of macrophages and fibroblasts. In this study, we hypothesized that exogenous interleukin-10 (IL-10), an anti-inflammatory cytokine, promotes post-MI repair through actions on these cardiac cell types. To test this hypothesis, C57BL/6J mice (male, 3- to 6-month old, $n = 24$/group) were treated with saline or IL-10 (50 μg/kg/day) by osmotic mini-pump infusion starting at day (d) 1 post-MI and sacrificed at d7 post-MI. IL-10 infusion doubled plasma IL-10 concentrations by d7 post-MI. Despite similar infarct areas and mortality rates, IL-10 treatment significantly decreased LV dilation (1.6-fold for end-systolic volume and 1.4-fold for end-diastolic volume) and improved ejection fraction 1.8-fold (both $p < 0.05$). IL-10 treatment attenuated inflammation at d7 post-MI, evidenced by decreased numbers of Mac-3+ macrophages in the infarct ($p < 0.05$). LV macrophages isolated from d7 post-MI mice treated with IL-10 showed significantly elevated gene expression of M2 markers (Arg1, Ym1, and TGF-β1; all $p < 0.05$). We further performed RNA-seq analysis on post-MI cardiac macrophages and identified 410 significantly different genes (155 increased, 225 decreased by IL-10 treatment). By functional network analysis grouping, the majority of genes (133 out of 410) were part of the cellular assembly and repair functional group. Of these, hyaluronidase 3 (Hyal3) is the most important feature identified by p value. IL-10 treatment decreased Hyal3 by 28%, which reduced hyaluronan degradation and limited collagen deposition (all $p < 0.05$). In addition, ex vivo IL-10 treatment increased fibroblast activation (proliferation, migration, and collagen production), an effect that was both directly and indirectly influenced by macrophage M2 polarization. Combined, our results

Correspondence to: Merry L. Lindsey.

Compliance with ethical standards

Conflict of interest The authors declare that they have no conflict of interest.

indicate that in vivo infusion of IL-10 post-MI improves the LV microenvironment to dampen inflammation and facilitate cardiac wound healing.

Keywords

IL-10; Macrophage; Fibroblast; Myocardial infarction; Inflammation; Collagen; Hyaluronan

Introduction

Following myocardial infarction (MI), the left ventricle (LV) undergoes a series of repair and wound healing responses that include inflammation and scar formation; the combined constituents are collectively termed LV remodeling. The extent of LV remodeling post-MI, in terms of both quality and quantity, determines long-term outcomes that include LV structure and function and chronic survival rates [10]. Excessive and extended LV remodeling can progress to heart failure post-MI, and the 5-year mortality rate for heart failure approaches 50% [36, 53]. Accordingly, there is a need to better understand the cellular and molecular mechanisms that regulate post-MI LV remodeling.

After MI, there is robust leukocyte infiltration into the infarct area to clear necrotic debris. As an innate stress response against myocardial injury, proinflammatory cytokines such as tumor necrosis factor (TNF)-α, Interleukin (IL)-1 beta (β), and IL-6 are increased within 1 h post-MI [37]. By days 3–5 post-MI, the inflammatory reaction transitions to an anti-inflammatory reparative response, characterized by the accelerated activation and proliferation of fibroblasts [5, 15, 52]. While inflammation is a necessary component during the early stage of LV remodeling, a prolonged inflammatory response may impair LV physiology by promoting LV dilation and excessive scar formation [13]. Therefore, timely resolution of the inflammatory response is a critical juncture of remodeling. At days 1–7 post-MI, reparative macrophages are recruited and release inhibitory mediators such as transforming growth factor (TGF)-β and IL-10, which suppress inflammation and activate profibrotic processes [11].

IL-10 is an anti-inflammatory cytokine with a strong capacity to suppress proinflammation [14, 57]. In animal models, IL-10 is significantly increased in the serum within 6 h after myocardial ischemia/reperfusion [14]. In a variety of cell types, IL-10 inhibits the release of proinflammatory mediators [4, 38, 41]. In patients with acute MI, higher serum IL-10 within 24 h after angioplasty is associated with reduced incidence of heart failure progression [9]. After MI, IL-10-deficient mice have increased infarct size and enhanced myocardial necrosis with increased neutrophil infiltration [56]. Following MI, IL-10 treatment reduces inflammation and improves LV physiology [25]. In the current study, we investigated the cellular and molecular mechanisms responsible for the protective actions of IL-10 on post-MI LV remodeling.

Methods

Mice and treatment

The experimental design is shown in Fig. 1a. All animal procedures were approved by the Institutional Animal Care and Use Committee at the University of Mississippi Medical Center according to the Guide for the Care and Use of Laboratory Animals (Eighth edition, 2011). C57BL/6J WT male mice of 3–6 months were used in this study. All mice were kept in the same room in a light-controlled environment with a 12:12 h light–dark cycle and with free access to standard mouse chow and water. All mice were subjected to permanent left coronary artery ligation as previously described [59]. At day (d) 1 post-MI, myocardial infarction (MI) was confirmed by echocardiography, and saline or IL-10 (50 μg/kg/day) was infused subcutaneously via osmotic pumps. Non-surviving mice underwent autopsy, and surviving mice were sacrificed at d7 post-MI. At autopsy, cardiac rupture was affirmed by the presence of coagulated blood in the thoracic cavity or observation of the ruptured site on the LV. For all procedures, samples were randomized and analyzed in a blinded manner.

Echocardiography

To assess LV physiology, echocardiography was performed using a Vevo 2100™ system (VisualSonics, Toronto, ON, Canada) with a 30 MHz image transducer. Images were acquired prior to MI surgery (baseline) and at d1 and d7 post-MI. Mice were anesthetized with 1–2% isoflurane in an oxygen mix. Heart rate, body temperature, and electrocardiogram were monitored throughout the imaging procedure. Measurements were taken from the LV parasternal long axis (B-mode) and short axis (M-mode) views. For analysis, three images from consecutive cardiac cycles were analyzed and averaged. All images were acquired at heart rates >400 bpm [59].

Tissue harvest and infarct area evaluation

At d7 post-MI, all surviving mice were sacrificed, and the LV was collected as described previously [22]. Mice were anesthetized with 1–2% isoflurane in an oxygen mix, and blood was collected from the common carotid artery 5 min after heparin administration (4 U/g body weight, i.p.). The heparinized blood was immediately centrifuged for collection of plasma. Proteinase inhibitor cocktail (Roche, 50-720-4060, 1×) was added to the plasma, which was stored at −80 °C.

For tissue collection, the heart was flushed with cardioplegic solution (NaCl, 69 mM; $NaHCO_3$, 12 mM; glucose, 11 mM; 2,3-butanedione monoxime, 30 mM; EGTA, 10 mM; Nifedipine, 0.001 mM; KCl, 50 mM) to arrest the heart in diastole. LV and right ventricle (RV) were separated and weighed individually. Lung and tibia were collected and weighed. The LV was sliced into apex, middle, and base sections, stained with 1% 2, 3, 5-triphenyltetra-zolium chloride (Sigma), and imaged for calculation of infarct area. The LV infarct (LVI) was calculated using Photoshop (Adobe) and is presented as percentage of infarct area to total LV area [16]. The LVI and LVC were separated and individually snap frozen and stored at −80 °C for real- time RT^2-PCR analysis or immunoblotting analysis. The LV middle section was fixed in 10% zinc formalin (Fisher Scientific), paraffin-embedded, and sectioned for histological examination.

Immunohistochemistry

The middle part of the LV was paraffin-embedded and sectioned at 5 μm [30]. After rehydration, heat-mediated antigen retrieval was performed using the Target Retrieval Solution (S1699, Dako). The sections were incubated with 3% H_2O_2 (Sigma) to block endogenous peroxidase activity, followed by blocking with normal serum. A primary antibody specific for macrophages (Mac-3, Cedarlane CL8943AP; 1:100) was used at 4 °C overnight, followed by incubation with rabbit anti-rat IgG and ABC reagent (Vector Laboratories). The HistoMark Black peroxidase kit (Vector Laboratories) was used for positive staining of Mac-3, and eosin was used as a counterstain.

To examine whether the d7 post-MI macrophages were proliferative, multiplexed immunofluorescence was performed using the Opal Multiplex Immunohistochemistry Kit (Perkin Elmer) [50]. After rehydration, heat-mediated antigen retrieval was performed. Tissue sections were incubated with a primary antibody specific for macrophages (Mac-3) at 4 °C for 1 h, followed by incubation with a horseradish peroxidase (hrp)-conjugated anti-rat secondary antibody. A second primary antibody for proliferating cell nuclear antigen (PCNA, Abcam ab18197; 1:4000) was incubated at 4 °C for 1 h, followed by incubation with a hrp-conjugated anti-rabbit secondary antibody (for the PCNA primary Ab). After 10-min incubation, opal fluorophores were used to detect fluorescent signal, with the opal 570 fluorophore used for Mac-3 and the opal 690 fluorophore for PCNA. Staining with 4′,6-diamidino-2-phenylindole (DAPI) was used to stain nuclei. Non-specific binding was assessed by performing a no primary antibody control, and cross-over staining was assessed by performing each primary antibody staining on its own section. Images were acquired on the Mantra™ Quantitative Pathology Imaging microscope.

To determine collagen deposition in the infarct region, picrosirius red staining was performed using paraffin-sectioned LV tissue. Images from the infarct region were captured at 40× magnification with Image-Pro software (Media Cybernetics, Bethesda, MD, USA) and quantification was performed to calculate the percentage of positively stained area to total tissue area. A total of five images was acquired from each section ($n = 7$ saline and five IL10 sections).

Immunofluorescent staining was performed to evaluate the phenotype of the isolated cardiac fibroblasts. The fibroblasts were fixed with 4% paraformaldehyde and rinsed with sterile PBS, followed by blocking with goat serum. After blocking, the cells were incubated overnight at 4 °C with a primary antibody to α -smooth muscle actin (Abcam, ab32575, 1:100). The cells were rinsed in PBS and incubated with an anti-mouse secondary antibody (Vector Laboratories, BA-2001, 1:200) for 1 h at room temperature. The cells were washed with PBS, and incubated with Alexa Fluor 488 streptavidin (Life Technologies, S11223, 1:200). After PBS rinse, slides were cover slipped with Vectashield mounting media with Dapi (Vector H-1200) to stain nuclei. The signal intensity was analyzed by quantification of fluorescence intensity.

Cell isolation and stimulation

Macrophages and cardiac fibroblasts were isolated from the infarcted LV at d7 post-MI, and cardiac fibroblasts were also isolated from control no MI LV. As previously described [58], the LV was rinsed with PBS and the LVI was digested in collagenase solution (600 U/mL Collagenase II + 60 U/mL DNase I), followed by removal of erythrocytes using red cell lysis buffer (Miltenyi Biotec). Single cells were separated with pre-separation filters (Miltenyi Biotec 130-041-407, 30 μm) and the cellular pellet was resuspended in PEB buffer (PBS containing 2 mM EDTA and 0.5% BSA). Single cell suspensions were incubated serially with anti-Ly-6G MicroBead Kit mouse (10 min, Miltenyi Biotec, 130-092-332) and CD11b MicroBeads mouse/human (Miltenyi Biotec, 130-049-601) and isolated using a MiniMACS magnetic separator column. The effluent containing Ly-6G negative CD11b-positive macrophages were resuspended in 1 mL of RPMI 1640 media and plated in a 6-well plate (1.0×10^5 cells/well). The rest of the cells (Ly-6G negative, CD11b negative fibroblasts) were resuspended in 1 mL of Dulbecco's Modified Eagle's Medium (DMEM) supplemented with 10% FBS and plated in a 6-well plate (1.0×10^5 cells/well).

For isolation of peritoneal macrophages, 10 mL of ice-cold RPMI1640 media (Life technologies) with 10% fetal bovine serum (FBS, Life Technologies) and 1% antibiotics (Life Technologies) was injected into the peritoneal cavity of isoflurane-anesthetized mice (macrophages were resident cells and were not elicited). Media-containing cells were removed from the peritoneal cavity and centrifuged at 10009g for 10 min. The cell pellet was resuspended with RPMI1640 media, and the separated single cells were seeded in a 6-well plate (1×10^6 cells/well) and incubated at 37 °C for 18 h to attach. After 5 h, the media were replaced with new media and stimulated with recombinant mouse IL-10 (rIL-10; 50 ng/mL).

Real-Time RT-PCR and RNA-Seq

We extracted RNA from LVI tissue and from isolated macrophages as previously described [30]. RNA extraction was performed using TRIzol® Reagent (Invitrogen Life Technologies, Grand Island, NY, USA) according to manufacturer's instructions. RT2 First-Strand Kit (Qiagen, Valencia, CA, USA) was used for reverse transcription of RNA (0.4 μg). The gene expression levels of M1 markers (Ccl3, Ccl5, Il-1b, Il-6, Tnf-α) and for M2 markers (Arg1, Mrc1, Tgfb-1, Ym-1, Fizz-1) were measured by Taqman gene array analysis. Hypoxanthine guanine phosphoribosyl transferase 1 (Hprt1) gene was used as the reference gene for normalization.

To demonstrate the effect of IL-10 on post-MI LV macrophages, whole transcriptome analysis by RNA-seq was performed as described previously [6, 29]. Briefly, samples passed quality parameters (minimum concentration and size range) and were used to develop RNA libraries ($n = 12$ pooled index samples) using the TruSeq Stranded Total RNA with Ribo-Zero Kit, Set A (FC-122-2501, San Diego, CA) according to manufacturer's instructions. Each sample was prepared using 1 μg total RNA. The resulting cDNA libraries were quantified using the Qubit system (Invitrogen, Carlsbad, CA) and checked for quality and size using the Experion DNA 1 K chip (BioRad, Hercules, CA). The fragment size generated library ranged from 200 to 500 bps with a peak at ~250 bps. A portion of each

library was diluted to 10 nM and stored at −20 °C, and 10 μL of 1.2–1.8 nM libraries were diluted and denatured. The libraries were sequenced using the NextSeq 500 High Output Kit (300 cycles-PE100) on the Illumina NextSeq 500 platform. The sequencing reads were automatically uploaded and evaluated for quality using Illumina BaseSpace Onsite Computing platform. Subsequently, Fastq sequence files were generated and analysis was performed using applications available on BaseSpace Onsite Computing platform, including TopHat Alignment (read mapping to reference genome-USCS-GRCm38/mm10, etc.). Clustering and correlation analysis were carried out using Metaboanalyst 3.0 software analysis package (http://www.metaboanalyst.ca). The top 50 ranked genes, by *p* value and fold-change, were selected for heat map analysis.

Cardiac fibroblast proliferation and migration assay

The BrdU cell proliferation assay was used to evaluate the in vivo effect of IL-10 on ex vivo proliferation of isolated LVI fibroblasts. [60] BrdU assays were performed as reported previously [55]. Briefly, plated primary cardiac fibroblasts were incubated with BrdU for 24 h, and newly synthesized DNA was quantified by the magnitude of absorbance (optical density, OD) at 450 nm.

For the migration assay, 4.0×10^4 cells were plated in 96-well plates containing gold film surface electrodes and cultured overnight. The cells were serum starved for 18 h, and the wound healing assay was performed using electric cell-substrate impedance sensing (ECIS®, Applied Biophysics), which is a real-time, label-free, impedance-based method to study the activities of cells grown in tissue culture. The rate of migration was measured as the impedance change as cells migrated and covered the electrode [27].

Protein extraction and immunoblotting

To extract protein from the LVI, LV tissue was homogenized in protein extraction reagent 4 (Sigma) with 19 protease inhibitor using the Power Gen 1000 Homogenizer (Fisher Scientific). The homogenized LV was centrifuged at 4700 rpm to remove debris. A Bradford assay (BioRad) was used to measure the concentration of protein. The extracted protein was stored at −80 °C.

SDS-PAGE and immunoblotting analysis of total protein (10 μg) were performed, as previously described [23]. Specific primary antibodies against Mac-3 (Cedarlane CL8943B, 1:500), collagen I (Cedarlane CL50141AP-1, 1:1000), collagen III (Cedarlane CL50341AP-1, 1:1000), fibronectin (Abcam ab1954, 1:2000), and hyaluronic acid (Abcam ab53842, 1:1000) were used. ImageQuant TL 8.1 analysis software (GE Healthcare, Waukesha, WI) was used to quantify densitometry. The intensity of every lane was normalized to the densitometry of the total protein for that lane, as an internal loading control.

Statistical analyses

All treatments and analyses were performed in a blinded manner. Data are presented as mean ± SEM. Survival rates were analyzed by Kaplan-Meier survival analysis and compared by log-rank test. Rupture rates were analyzed by Fisher's exact test. Two group comparisons

were analyzed by Students *t* test. Multiple group comparisons were analyzed using one-way ANOVA, followed by the Student Newman–Keuls when the Bartlett's variation test was passed, or using the non-parametric Kruskal–Wallis test, followed by Dunn post hoc test when the Bartlett's variation test did not pass. A value of $p < 0.05$ was considered statistically significant.

Results

IL-10 treatment improved post-MI LV physiology, without affecting 7d post-MI infarct area or survival rates

IL-10 gene expression in the LV infarct (LVI) was significantly elevated at d1 following MI and returned towards d0 pre-MI control levels by d3 post-MI (Fig. 1b). The IL-10 dose used was based on the dose previously used by the Kishore laboratory [25]. IL-10 infusion resulted in a doubling of the plasma concentration at d7 post-MI (Fig. 1c). IL-10 treatment did not affect survival, rupture rates, or infarct area at d7 post-MI. As shown in Fig. 1d, 13 out of 24 saline-treated mice (54%) survived 7 days post-MI, and 10 out of 24 IL-10-treated mice survived (42%; $p = 0.45$). Cardiac rupture rates were similar between groups (6/11, 55% for saline and 7/14, 50% for IL-10; $p = 0.82$), which is consistent with the previous reports [48]. Infarct areas were comparable between MI groups: saline was 62 ± 2% and IL-10 was 60 ± 3% ($p = 0.61$, Fig. 1e). These results indicate that all mice received similar ischemic injuries. This was expected, as IL-10 infusion was started at d1 post-MI, after induction of infarction and after the time when myocardial salvage would be expected. In the absence of reperfusion, essentially all cardiomyocytes in the area at risk undergo cell death.

Despite similar survival rates and infarct area, IL-10 treatment improved LV physiology at d7 post-MI. IL-10 treatment reduced end-systolic volumes by 1.6-fold and end-diastolic volumes by 1.4-fold (both $p < 0.05$, Fig. 1f, g). IL-10 treatment improved ejection fraction by 1.8-fold compared to the saline group ($p < 0.05$, Fig. 1h). The attenuated dilation and improved ejection fraction indicated a protective role of IL-10 in post-MI LV remodeling.

IL-10 treatment promoted d7 LVI anti-inflammatory gene expression

Since IL-10 treatment significantly improved LV physiology and IL-10 is known to exert anti-inflammatory actions, we evaluated the d7 post-MI inflammatory response [12, 15]. Out of ten M1 or M2 genes evaluated (Ccl3, Ccl5, Il-1b, Il-6, Tnf-α, Arg1, Cd163, Mrc1, Tgf-b1, and Ym1), four genes were significantly elevated in IL-10-treated LVI compared to saline-treated LVI. Of these, three were anti-inflammatory (Arg1, Mrc1 and Tgfb1) and one was proinflammatory (Il1b; all $p < 0.05$, Fig. 2a, b). The altered genes associate with macrophage polarization and suggest that IL-10 treatment may skew macrophages towards anti-inflammatory (M2) phenotypes.

IL-10 treatment reduced macrophage numbers and stimulated M2 macrophage polarization

To evaluate the mechanisms whereby IL-10 altered polarization, we measured the mRNA expression of M1 (Ccl3, Ccl5, Il1b, Il6, and Tnfa) and M2 (Arg1, Cd163, Mrc1, Tgfb1, and Ym1) markers in macrophages isolated from d7 saline- or IL-10-treated LVI. While IL-10 treatment had no effect on the 5 M1 markers measured (Fig. 3a), IL-10 significantly elevated

three of the five M2 markers (Arg1, Tgfb1, and Ym1; all $p < 0.05$, Fig. 3b). Of note, these three markers are genes whose expression have been related to resolution of inflammation by inhibiting proinflammation.

To validate the effect of IL-10 on the inflammatory response, macrophage numbers in the infarct were counted. As assessed by immunohistochemical staining, IL-10 treatment significantly attenuated the number of mac-3^+ macrophages at d7 post-MI ($p < 0.05$, Fig. 3c).

To examine whether decreased macrophage numbers in the infarct with IL-10 treatment was due to a difference in proliferation rates, we dual-stained for macrophages (Mac-3) and proliferation (PCNA). None of the Mac-3 positive cells were PCNA-positive, indicating that proliferation did not account for the differences in cell numbers. This result is consistent with the past reports from the Nahrendorf laboratory, which showed that steady-state resident cardiac macrophages proliferate locally and self-renew, while circulating non-proliferative infiltrating monocytes contribute to the macrophage pool in the acute infarct [19]. These results indicate that IL-10 treatment enhanced M2 polarization and reduced macrophage numbers, leading to an overall anti-inflammatory response in the infarct region.

IL-10 down-regulated hyaluronidase 3 (Hyal3) in d7 post-MI cardiac macrophages

To comprehensively evaluate macrophage phenotypes, RNA-seq was used to compare macrophages isolated from saline- and IL-10-treated LVI. As shown in Fig. 4a, out of 23,350 genes evaluated, 410 genes were significantly different between saline and IL-10 groups (all $p < 0.05$). IL-10 treatment up-regulated 155 genes and down-regulated 255 genes compared to saline. The heat map of the top 50 ranked significantly different genes between saline- and IL-10-treated LVI macrophages is shown in Fig. 4b. Further functional network evaluation of these genes was performed with ingenuity pathway analysis (IPA; Qiagen Bioinformatics). The most represented group (133 out of the 410 genes, 32.4%) was the cellular assembly and repair functional group. In particular, IL-10 treatment significantly decreased Hyal3 by 28% (Fig. 4c). Hyal3 is an enzyme that degrades hyaluronic acid, a ubiquitous extracellular matrix (ECM) component whose degradation is associated with inflammatory response [8, 18, 24, 39]. Reduced Hyal3 gene expression in LVI macrophages from the IL-10 treatment group was confirmed by qPCR (Fig. 4d $p < 0.05$). We measured gene expression for 23 MMPs and 4 TIMPs in d7 post-MI isolated macrophages. There were no differences in expression for any of these 27 genes. We also evaluated MMP-2, MMP-9, and TIMP-1 protein in the LVI, and there were no differences between groups.

To validate whether decreased Hyal3 affects hyaluronic acid turnover in IL-10-treated LVI post-MI, we measured hyaluronic acid protein by immunoblotting. As shown in Fig. 4e, IL-10 treatment increased high molecular weight full-length hyaluronic acid in the LVI at d7 post-MI ($p < 0.05$) and reduced low molecular weight hyaluronic acid degradation fragments by IL-10 treatment. Full-length and hyaluronic acid fragments differentially affect macrophage activation and inflammation. While full-length hyaluronic acid activates macrophages to its enhance pro-resolving functions, hyaluronic acid fragments stimulate macrophages to induce a proinflammatory response [39, 44]. Our data reveal that IL-10 inhibited Hyal3 expression in cardiac macrophages, leading to reduced hyaluronic acid

degradation in the infarct. This could affect inflammation resolution by decreasing both numbers and M2 phenotype of the LVI macrophages.

IL-10 treatment enhances proliferation and migration of post-MI cardiac fibroblasts

After MI, there is cross-talk among multiple cardiac cell types involved in cardiac repair. Inflammation resolution is associated with fibroblast activation, and macrophages are regulators of this process [26, 42]. To explore cross-talk mechanisms between macrophages and fibroblasts, we stimulated control fibroblasts in vitro and isolated ex vivo d7 post-MI LVI macrophages and fibroblasts from saline-and IL-10-treated groups. To obtain post-MI macrophage conditioned media (secretome), D7 LVI macrophages were cultured for 16 h. d0 fibroblasts were stimulated with either the secretome of LVI macrophages or IL-10 and compared to d7 LVI fibroblasts.

IL-10 indirectly stimulated fibroblast activation through direct effects on macrophages. As shown in Fig. 5a, the secretome collected from cardiac macrophages isolated from IL-10-treated LVI stimulated both proliferation and migration compared to the secretome of macrophages isolated from saline-treated LVI (both $p < 0.05$). IL-10 showed no direct effect on cardiac fibroblasts, as control cardiac fibroblasts stimulated with IL-10 (50 ng/mL) had no effect on proliferation or migration (Fig. 5b). To determine whether in vitro stimulation with the post-MI macrophage secretome recapitulated the ex vivo phenotype, we evaluated cardiac fibroblasts from saline- and IL-10-treated d7 LVI. IL-10 in vivo treatment significantly increased ex vivo proliferation and migration rates, as well as up-regulated α-smooth muscle actin protein expression (all $p < 0.05$, Fig. 5c), indicating that macrophages regulated fibroblast cell physiology. Our results indicate that IL-10 induced M2 polarized macrophages to indirectly affect fibroblast differentiation.

IL-10 treatment reduced d7 post-MI ECM accumulation

By d7 post-MI, damaged myocytes are being replaced by new ECM to form the infarct scar. Since fibroblast activation was induced by IL-10 treatment, we evaluated ECM synthesis in d7 LVI fibroblasts by measuring collagen I and III secretion. Collagen I secretion, and not collagen III, was significantly reduced in IL-10-treated LVI fibroblasts compared to saline group ($p < 0.05$, Fig. 6a). IL-10 treatment, therefore, decreased the ratio of collagen I to collagen III.

To determine whether collagen secretion from cardiac fibroblasts affected overall ECM deposition in the infarct region, we measured collagen I and III protein in d7 LVI. IL-10 treatment decreased collagen I in the infarct without changing collagen III (Fig. 6b). Consistent with the ex vivo data, IL-10 treatment significantly reduced the ratio of collagen I to collagen III protein ($p < 0.05$, Fig. 6b). A reduced collagen I–III ratio is associated with reduced myocardial fibrosis, a major determinant of LV dysfunction [3]. Our results indicate that scar formation is optimized with IL-10 treatment (Fig. 6c, $p < 0.05$).

To explore whether the reduced collagen I–III ratio by IL-10 treatment affected scar formation, picrosirius red-stained sections were evaluated. LVI sections from IL-10-treated mice showed reduced collagen accumulation in the infarct, which could explain the improved cardiac physiology.

Discussion

The goal of this study was to evaluate the therapeutic applicability of IL-10 to improve post-MI wound healing through actions on macrophages and fibroblasts. Our results demonstrated that IL-10 infusion in vivo significantly improved post-MI cardiac physiology and increased M2 cardiac macrophage polarization and fibroblast activation to moderate collagen deposition. Our results reveal the mechanisms whereby IL-10 protects against adverse cardiac remodeling following MI, namely by decreasing inflammation and increasing wound healing properties through direct effects on macrophages and indirect effects on fibroblasts (Fig. 7).

IL-10 is a well-known anti-inflammatory cytokine that inhibits production of proinflammatory cytokines. In aged mice, IL-10 deficiency exaggerates LV dysfunction and inflammation [49]. In young mice, IL-10 deficiency has less impressive effects, despite significantly elevating myocardial TNF-α and CCL2 [61]. Exendin-4 elevated IL-10 expression, which was associated with a cardioprotective effect on post-MI cardiac remodeling [46]. Kishore et al. showed that subcutaneous injection of IL-10 post-MI reduced LV dysfunction and infarct wall thinning [25]. In concordance with results from the Kishore laboratory, IL-10 treatment improved LV function post-MI in our mice. Combined, our results and the literature support the idea that regulation of the inflammatory response by elevating IL-10 may provide cardioprotection to prevent adverse LV remodeling following MI. Whether endogenous IL-10 is sufficient to exert a critical effect on post-MI remodeling needs more investigation.

Macrophages play both beneficial and detrimental roles in the wound healing process after MI and, therefore, modulation of particular macrophage actions could be therapeutic to promote myocardial repair [20, 35]. Within several hours post-MI, the inflammatory response is activated with production of proinflammatory cytokines, also called as M1 cytokines [7, 26]. Following MI, M1 classically polarized macrophages dominate in the LV during the early proinflammatory stage, while during the later anti-inflammatory stage there is a transition to M2 alternatively polarized macrophages [21, 28, 51]. Promoting a timely transition from M1 proinflammation to M2 anti-inflammation may improve MI outcomes. IL-10 treatment induced M2 polarization of cardiac macrophages, leading to an infarct environment favorable to tissue repair.

The effects of IL-10 on cardiac macrophages are not limited to polarization to the M2 phenotype and include secretion of ECM modulators. Out of 23,350 genes sequenced in macrophages isolated from the infarct region, 410 genes were significantly different between saline- and IL-10-treated mice. Of these hyaluronidase, three showed the largest fold-change between groups. Hyaluronidase 3 is the enzyme that catalyzes hyaluronic acid fragmentation. While hyaluronidase activity has been detected in isolated rabbit lung alveolar macrophages [16], hyaluronidase activity has not been previously measured in cardiac macrophages. Our results indicate that IL-10 treatment stimulated inflammation resolution through a macrophage-dependent hyaluronidase-3/hyaluronic acid degradation mechanism.

In addition to coordinating inflammation, macrophages stimulate fibroblast activation, as paracrine factors of M1 or M2 polarized macrophages stimulated distinct fibroblast phenotypes [43]. The M2 macrophage, in particular, associates with tissue repair and fibroblast activation [33, 34, 54]. IL-10 induced M2 macrophage polarization, and the M2 macrophage secretome activated cardiac fibroblasts, indicating the presence of cross-talk between macrophages and fibroblasts in the infarct. While IL-10 had no direct effect on cardiac fibroblasts, IL-10 induced M2 macrophages to secrete factors that increased fibroblast activation, indicating a strong contribution for cross-talk between these two cell types.

Activated fibroblasts generate contractile forces to reorganize extracellular matrix (ECM) and this procedure determines the quality of infarct scar either good scar or fibrosis. Although ECM deposition is required for scar formation and prevents wall thinning and rupture following MI, excessive accumulation of ECM and an increased ratio of collagen I to III both associate with increased LV wall stiffness [17, 31, 32, 47]. In patients with cardiomyopathy, increased collagen I, but not collagen III, associated with systolic and diastolic dysfunction [40]. The fibroblast cell number affects collagen metabolism; specifically, collagen I synthesis decreases as fibroblast numbers pass a threshold density [45]. Myofibroblast transdifferentiation does not necessarily lead to increased collagen deposition. When myofibroblasts are highly proliferative, collagen production is actually dampened to balance collagen synthesis and degradation [1]. Higher hyaluronan is consistent with this finding, as higher hyaluronan in dermal tissue associates with increased fibroblast activation and less collagen scar formation [2]. Our results suggest that the myofibroblast activation stimulated by IL-10 infusion is a hyper-activated state represented by enriched hyaluronan and reduced collagen. Taken together, our results indicate that IL-10 treatment significantly reduced myocardial fibrosis post-MI by increasing proliferation of fibroblasts to decrease the collagen I to III ratio.

It is possible that administration of IL-10 in the presence of a permanently occluded coronary artery may have resulted in uneven delivery of IL-10 into the infarcted myocardium. While the kinetics and distribution of IL-10 entry into the infarcted myocardium were not evaluated in this study, based on LV physiology and inflammatory responses, early effects were noted. Following MI, increased recruitment of blood monocyte into the infarct is associated with adverse cardiac remodeling and promoted left ventricular dilatation [35]. In this study, circulating cells were not evaluated.

In conclusion, the present study established a better mechanistic understanding of the cardioprotective role of IL-10 in the post-MI LV. Our results indicate that in vivo infusion of IL-10 post-MI improves the LV microenvironment to decrease inflammation and facilitate healing.

Acknowledgments

Research reported in this publication was supported by the American Heart Association under Award Number 15SDG22930009, by the National Heart, Lung, and Blood Institute and the National Institute of General Medical Sciences of the National Institutes of Health under Award Numbers HL075360, HL129823, HL051971, GM104357, GM114833, and GM115428, and from the Biomedical Laboratory Research and Development Service of the Veterans Affairs Office of Research and Development under Award Number 5I01BX000505. The content is

solely the responsibility of the authors and does not necessarily represent the official views of the American Heart Association, the National Institutes of Health, or the Veterans Administration.

References

1. Abe S, Steinmann BU, Wahl LM, Martin GR. High cell density alters the ratio of type III to I collagen synthesis by fibroblasts. Nature. 1979; 279:442–444. DOI: 10.1038/279442a0 [PubMed: 16068188]
2. Balaji S, King A, Marsh E, LeSaint M, Bhattacharya SS, Han N, Dhamija Y, Ranjan R, Le LD, Bollyky PL, Crombleholme TM, Keswani SG. The role of interleukin-10 and hyaluronan in murine fetal fibroblast function in vitro: implications for recapitulating fetal regenerative wound healing. PLoS One. 2015; 10:e0124302.doi: 10.1371/journal.pone.0124302 [PubMed: 25951109]
3. Beam J, Botta A, Ye J, Soliman H, Matier BJ, Forrest M, MacLeod KM, Ghosh S. Excess linoleic acid increases collagen I/III ratio and “stiffens” the heart muscle following high fat diets. J Biol Chem. 2015; 290:23371–23384. DOI: 10.1074/jbc.M115.682195 [PubMed: 26240151]
4. Berg DJ, Kuhn R, Rajewsky K, Muller W, Menon S, Davidson N, Grunig G, Rennick D. Interleukin-10 is a central regulator of the response to LPS in murine models of endotoxic shock and the Shwartzman reaction but not endotoxin tolerance. J Clin Investig. 1995; 96:2339–2347. DOI: 10.1172/JCI118290 [PubMed: 7593621]
5. Christia P, Bujak M, Gonzalez-Quesada C, Chen W, Dobaczewski M, Reddy A, Frangogiannis NG. Systematic characterization of myocardial inflammation, repair, and remodeling in a mouse model of reperfused myocardial infarction. J Histochem Cytochem. 2013; 61:555–570. DOI: 10.1369/0022155413493912 [PubMed: 23714783]
6. Cobos Jimenez V, Bradley EJ, Willemsen AM, van Kampen AH, Baas F, Kootstra NA. Next-generation sequencing of microRNAs uncovers expression signatures in polarized macrophages. Physiol Genomics. 2014; 46:91–103. DOI: 10.1152/physiolgenomics.00140.2013 [PubMed: 24326348]
7. de Couto G, Liu W, Tseliou E, Sun B, Makkar N, Kanazawa H, Arditi M, Marban E. Macrophages mediate cardioprotective cellular postconditioning in acute myocardial infarction. J Clin Investig. 2015; 125:3147–3162. DOI: 10.1172/JCI81321 [PubMed: 26214527]
8. de Sa VK, Olivieri E, Parra ER, Ab’Saber AM, Takagaki T, Soares FA, Carraro D, Carvalho L, Capelozzi VL. Hyaluronidase splice variants are associated with histology and outcome in adenocarcinoma and squamous cell carcinoma of the lung. Hum Pathol. 2012; 43:675–683. DOI: 10.1016/j.humpath.2011.06.010 [PubMed: 21992818]
9. Dominguez Rodriguez A, Abreu Gonzalez P, Garcia Gonzalez MJ, Ferrer Hita J. Association between serum interleukin 10 level and development of heart failure in acute myocardial infarction patients treated by primary angioplasty. Rev Esp Cardiol (Engl Ed). 2005; 58:626–630. DOI: 10.1016/S1885-5857(06)60248-X
10. Frangogiannis NG. The immune system and cardiac repair. Pharmacol Res. 2008; 58:88–111. DOI: 10.1016/j.phrs.2008.06.007 [PubMed: 18620057]
11. Frangogiannis NG. Inflammation in cardiac injury, repair and regeneration. Curr Opin Cardiol. 2015; 30:240–245. DOI: 10.1097/HCO.0000000000000158 [PubMed: 25807226]
12. Frangogiannis NG. Regulation of the inflammatory response in cardiac repair. Circ Res. 2012; 110:159–173. DOI: 10.1161/CIRCRESAHA.111.243162 [PubMed: 22223212]
13. Frangogiannis NG. Targeting the inflammatory response in healing myocardial infarcts. Curr Med Chem. 2006; 13:1877–1893. DOI: 10.2174/092986706777585086 [PubMed: 16842199]
14. Frangogiannis NG, Mendoza LH, Lindsey ML, Ballantyne CM, Michael LH, Smith CW, Entman ML. IL-10 is induced in the reperfused myocardium and may modulate the reaction to injury. J Immunol. 2000; 165:2798–2808. DOI: 10.4049/jimmunol.165.5.2798 [PubMed: 10946312]
15. Frangogiannis NG, Smith CW, Entman ML. The inflammatory response in myocardial infarction. Cardiovasc Res. 2002; 53:31–47. DOI: 10.1016/S0008-6363(01)00434-5 [PubMed: 11744011]
16. Goggins JF, Lazarus GS, Fullmer HM. Hyaluronidase activity of alveolar macrophages. J Histochem Cytochem. 1968; 16:688–692. DOI: 10.1177/16.11.688 [PubMed: 5723776]

17. Goldberg MT, Han YP, Yan C, Shaw MC, Garner WL. TNF-alpha suppresses alpha-smooth muscle actin expression in human dermal fibroblasts: an implication for abnormal wound healing. J Investig Dermatol. 2007; 127:2645–2655. DOI: 10.1038/sj.jid.5700890 [PubMed: 17554369]
18. Hasan AS, Luo L, Yan C, Zhang TX, Urata Y, Goto S, Mangoura SA, Abdel-Raheem MH, Zhang S, Li TS. Cardiosphere-derived cells facilitate heart repair by modulating M1/M2 macrophage polarization and neutrophil recruitment. PLoS One. 2016; 11:e0165255.doi: 10.1371/journal.pone.0165255 [PubMed: 27764217]
19. Heidt T, Courties G, Dutta P, Sager HB, Sebas M, Iwamoto Y, Sun Y, Da Silva N, Panizzi P, van der Laan AM, Swirski FK, Weissleder R, Nahrendorf M. Differential contribution of monocytes to heart macrophages in steady-state and after myocardial infarction. Circ Res. 2014; 115:284–295. DOI: 10.1161/CIRCRESAHA.115.303567 [PubMed: 24786973]
20. Ismahil MA, Hamid T, Bansal SS, Patel B, Kingery JR, Prabhu SD. Remodeling of the mononuclear phagocyte network underlies chronic inflammation and disease progression in heart failure: critical importance of the cardiosplenic axis. Circ Res. 2014; 114:266–282. DOI: 10.1161/CIRCRESAHA.113.301720 [PubMed: 24186967]
21. Italiani P, Boraschi D. From monocytes to M1/M2 macrophages: phenotypical vs. functional differentiation. Front Immunol. 2014; 5:514.doi: 10.3389/fimmu.2014.00514 [PubMed: 25368618]
22. Iyer RP, de Castro Bras LE, Cannon PL, Ma Y, DeLeon-Pennell KY, Jung M, Flynn ER, Henry JB, Bratton DR, White JA, Fulton LK, Grady AW, Lindsey ML. Defining the sham environment for post-myocardial infarction studies in mice. Am J Physiol Heart Circ Physiol. 2016; 311:H822–H836. DOI: 10.1152/ajpheart.00067.2016 [PubMed: 27521418]
23. Iyer RP, Patterson NL, Zouein FA, Ma Y, Dive V, de Castro Bras LE, Lindsey ML. Early matrix metalloproteinase-12 inhibition worsens post-myocardial infarction cardiac dysfunction by delaying inflammation resolution. Int J Cardiol. 2015; 185:198–208. DOI: 10.1016/j.ijcard.2015.03.054 [PubMed: 25797678]
24. Kim Y, Kumar S. CD44-mediated adhesion to hyaluronic acid contributes to mechanosensing and invasive motility. Mol Cancer Res. 2014; 12:1416–1429. DOI: 10.1158/1541-7786.MCR-13-0629 [PubMed: 24962319]
25. Krishnamurthy P, Rajasingh J, Lambers E, Qin G, Losordo DW, Kishore R. IL-10 inhibits inflammation and attenuates left ventricular remodeling after myocardial infarction via activation of STAT3 and suppression of HuR. Circ Res. 2009; 104:e9–18. DOI: 10.1161/CIRCRESAHA.108.188243 [PubMed: 19096025]
26. Lambert JM, Lopez EF, Lindsey ML. Macrophage roles following myocardial infarction. Int J Cardiol. 2008; 130:147–158. DOI: 10.1016/j.ijcard.2008.04.059 [PubMed: 18656272]
27. Lindsey ML, Iyer RP, Zamilpa R, Yabluchanskiy A, DeLeon-Pennell KY, Hall ME, Kaplan A, Zouein FA, Bratton D, Flynn ER, Cannon PL, Tian Y, Jin YF, Lange RA, Tokmina-Roszyk D, Fields GB, de Castro Bras LE. A novel collagen matri-cryptin reduces left ventricular dilation post-myocardial infarction by promoting scar formation and angiogenesis. J Am Coll Cardiol. 2015; 66:1364–1374. DOI: 10.1016/j.jacc.2015.07.035 [PubMed: 26383724]
28. Lindsey ML, Saucerman JJ, DeLeon-Pennell KY. Knowledge gaps to understanding cardiac macrophage polarization following myocardial infarction. Biochim Biophys Acta. 2016; 1862:2288–2292. DOI: 10.1016/j.bbadis.2016.05.013 [PubMed: 27240543]
29. Liu GW, Livesay BR, Kacherovsky NA, Cieslewicz M, Lutz E, Waalkes A, Jensen MC, Salipante SJ, Pun SH. Efficient identification of murine M2 macrophage peptide targeting ligands by phage display and next-generation sequencing. Bioconjug Chem. 2015; 26:1811–1817. DOI: 10.1021/acs.bioconjchem.5b00344 [PubMed: 26161996]
30. Ma Y, Chiao YA, Clark R, Flynn ER, Yabluchanskiy A, Ghasemi O, Zouein F, Lindsey ML, Jin YF. Deriving a cardiac ageing signature to reveal MMP-9-dependent inflammatory signalling in senescence. Cardiovasc Res. 2015; 106:421–431. DOI: 10.1093/cvr/cvv128 [PubMed: 25883218]
31. Ma Y, de Castro Bras LE, Toba H, Iyer RP, Hall ME, Winniford MD, Lange RA, Tyagi SC, Lindsey ML. Myofibroblasts and the extracellular matrix network in post-myocardial infarction cardiac remodeling. Pflugers Arch. 2014; 466:1113–1127. DOI: 10.1007/s00424-014-1463-9 [PubMed: 24519465]

32. Ma Y, Halade GV, Lindsey ML. Extracellular matrix and fibroblast communication following myocardial infarction. J Cardiovasc Transl Res. 2012; 5:848–857. DOI: 10.1007/s12265-012-9398-z [PubMed: 22926488]
33. Martin P, Leibovich SJ. Inflammatory cells during wound repair: the good, the bad and the ugly. Trends Cell Biol. 2005; 15:599–607. DOI: 10.1016/j.tcb.2005.09.002 [PubMed: 16202600]
34. Murray PJ, Wynn TA. Obstacles and opportunities for understanding macrophage polarization. J Leukoc Biol. 2011; 89:557–563. DOI: 10.1189/jlb.0710409 [PubMed: 21248152]
35. Nahrendorf M, Pittet MJ, Swirski FK. Monocytes: protagonists of infarct inflammation and repair after myocardial infarction. Circulation. 2010; 121:2437–2445. DOI: 10.1161/CIRCULATIONAHA.109.916346 [PubMed: 20530020]
36. Nahrendorf M, Wiesmann F, Hiller KH, Hu K, Waller C, Ruff J, Lanz TE, Neubauer S, Haase A, Ertl G, Bauer WR. Serial cine-magnetic resonance imaging of left ventricular remodeling after myocardial infarction in rats. J Magn Reson Imaging. 2001; 14:547–555. DOI: 10.1002/jmri.1218 [PubMed: 11747006]
37. Nian M, Lee P, Khaper N, Liu P. Inflammatory cytokines and postmyocardial infarction remodeling. Circ Res. 2004; 94:1543–1553. DOI: 10.1161/01.RES.0000130526.20854.fa [PubMed: 15217919]
38. Ocuin LM, Bamboat ZM, Balachandran VP, Cavnar MJ, Obaid H, Plitas G, DeMatteo RP. Neutrophil IL-10 suppresses peritoneal inflammatory monocytes during polymicrobial sepsis. J Leukoc Biol. 2011; 89:423–432. DOI: 10.1189/jlb.0810479 [PubMed: 21106642]
39. Papakonstantinou E, Roth M, Karakiulakis G. Hyaluronic acid: a key molecule in skin aging. Dermatoendocrinology. 2012; 4:253–258. DOI: 10.4161/derm.21923
40. Pauschinger M, Knopf D, Petschauer S, Doerner A, Poller W, Schwimmbeck PL, Kuhl U, Schultheiss HP. Dilated car-diomyopathy is associated with significant changes in collagen type I/III ratio. Circulation. 1999; 99:2750–2756. DOI: 10.1161/01.CIR.99.21.2750 [PubMed: 10351968]
41. Perretti M, Szabo C, Thiemermann C. Effect of inter-leukin-4 and interleukin-10 on leucocyte migration and nitric oxide production in the mouse. Br J Pharmacol. 1995; 116:2251–2257. DOI: 10.1111/j.1476-5381.1995.tb15061.x [PubMed: 8564256]
42. Pinto AR, Godwin JW, Rosenthal NA. Macrophages in cardiac homeostasis, injury responses and progenitor cell mobilisation. Stem Cell Res. 2014; 13:705–714. DOI: 10.1016/j.scr.2014.06.004 [PubMed: 25087895]
43. Ploeger DT, Hosper NA, Schipper M, Koerts JA, de Rond S, Bank RA. Cell plasticity in wound healing: paracrine factors of M1/M2 polarized macrophages influence the pheno-typical state of dermal fibroblasts. Cell Commun Signal. 2013; 11:29.doi: 10.1186/1478-811X-11-29 [PubMed: 23601247]
44. Rayahin JE, Buhrman JS, Zhang Y, Koh TJ, Gemeinhart RA. High and low molecular weight hyaluronic acid differentially influence macrophage activation. ACS Biomater Sci Eng. 2015; 1:481–493. DOI: 10.1021/acsbiomaterials.5b00181 [PubMed: 26280020]
45. Redden RA, Doolin EJ. Collagen crosslinking and cell density have distinct effects on fibroblast-mediated contraction of collagen gels. Skin Res Technol. 2003; 9:290–293. DOI: 10.1034/j.1600-0846.2003.00023.x [PubMed: 12877693]
46. Robinson E, Cassidy RS, Tate M, Zhao Y, Lockhart S, Calder-wood D, Church R, McGahon MK, Brazil DP, McDermott BJ, Green BD, Grieve DJ. Exendin-4 protects against post-myocardial infarction remodelling via specific actions on inflammation and the extracellular matrix. Basic Res Cardiol. 2015; 110:20.doi: 10.1007/s00395-015-0476-7 [PubMed: 25725809]
47. Rolfe KJ, Grobbelaar AO. A review of fetal scarless healing. ISRN Dermatol. 2012; 2012:698034.doi: 10.5402/2012/698034 [PubMed: 22675640]
48. Salto-Tellez M, Yung Lim S, El-Oakley RM, Tang TP, ALmsherqi ZAM, Lim SK. Myocardial infarction in the C57BL/6J mouse: a quantifiable and highly reproducible experimental model. Cardiovasc Pathol. 2004; 13:91–97. DOI: 10.1016/S1054-8807(03)00129-7 [PubMed: 15033158]
49. Sikka G, Miller KL, Steppan J, Pandey D, Jung SM, Fraser CD 3rd, Ellis C, Ross D, Vandegaer K, Bedja D, Gabrielson K, Walston JD, Berkowitz DE, Barouch LA. Interleukin 10 knockout frail

mice develop cardiac and vascular dysfunction with increased age. Exp Gerontol. 2013; 48:128–135. DOI: 10.1016/j.exger.2012.11.001 [PubMed: 23159957]

50. Stack EC, Foukas PG, Lee PP. Multiplexed tissue biomarker imaging. J Immunother Cancer. 2016; 4:9.doi: 10.1186/s40425-016-0115-3 [PubMed: 26885371]
51. ter Horst EN, Hakimzadeh N, van der Laan AM, Krijnen PA, Niessen HW, Piek JJ. Modulators of macrophage polarization influence healing of the infarcted myocardium. Int J Mol Sci. 2015; 16:29583–29591. DOI: 10.3390/ijms161226187 [PubMed: 26690421]
52. Turillazzi E, Di Paolo M, Neri M, Riezzo I, Fineschi V. A theoretical timeline for myocardial infarction: immunohistochemical evaluation and western blot quantification for Inter-leukin-15 and Monocyte chemotactic protein-1 as very early markers. J Transl Med. 2014; 12:188.doi: 10.1186/1479-5876-12-188 [PubMed: 24989171]
53. White HD, Norris RM, Brown MA, Brandt PW, Whitlock RM, Wild CJ. Left ventricular end-systolic volume as the major determinant of survival after recovery from myocardial infarction. Circulation. 1987; 76:44–51. DOI: 10.1161/01.CIR.76.1.44 [PubMed: 3594774]
54. Wynn TA, Barron L. Macrophages: master regulators of inflammation and fibrosis. Semin Liver Dis. 2010; 30:245–257. DOI: 10.1055/s-0030-1255354 [PubMed: 20665377]
55. Xia H, Diebold D, Nho R, Perlman D, Kleidon J, Kahm J, Avdulov S, Peterson M, Nerva J, Bitterman P, Henke C. Pathological integrin signaling enhances proliferation of primary lung fibroblasts from patients with idiopathic pulmonary fibrosis. J Exp Med. 2008; 205:1659–1672. DOI: 10.1084/jem.20080001 [PubMed: 18541712]
56. Yang Z, Zingarelli B, Szabo C. Crucial role of endogenous interleukin-10 production in myocardial ischemia/reperfusion injury. Circulation. 2000; 101:1019–1026. DOI: 10.1161/01.CIR.101.9.1019 [PubMed: 10704170]
57. Yao L, Huang K, Huang D, Wang J, Guo H, Liao Y. Acute myocardial infarction induced increases in plasma tumor necrosis factor-alpha and interleukin-10 are associated with the activation of poly(ADP-ribose) polymerase of circulating mononuclear cell. Int J Cardiol. 2008; 123:366–368. DOI: 10.1016/j.ijcard.2007.06.069 [PubMed: 17689746]
58. Zamilpa R, Ibarra J, de Castro Bras LE, Ramirez TA, Nguyen N, Halade GV, Zhang J, Dai Q, Dayah T, Chiao YA, Lowell W, Ahuja SS, D'Armiento J, Jin YF, Lindsey ML. Transgenic overexpression of matrix metalloproteinase-9 in macrophages attenuates the inflammatory response and improves left ventricular function post-myocardial infarction. J Mol Cell Cardiol. 2012; 53:599–608. DOI: 10.1016/j.yjmcc.2012.07.017 [PubMed: 22884843]
59. Zamilpa R, Zhang J, Chiao YA, de Castro Bras LE, Halade GV, Ma Y, Hacker SO, Lindsey ML. Cardiac wound healing post-myocardial infarction: a novel method to target extracellular matrix remodeling in the left ventricle. Methods Mol Biol. 2013; 1037:313–324. DOI: 10.1007/978-1-62703-505-7_18 [PubMed: 24029944]
60. Zheng JL, Helbig C, Gao WQ. Induction of cell proliferation by fibroblast and insulin-like growth factors in pure rat inner ear epithelial cell cultures. J Neurosci. 1997; 17:216–226. DOI: 10.1073/pnas.92.8.3152 [PubMed: 8987750]
61. Zymek P, Nah DY, Bujak M, Ren G, Koerting A, Leucker T, Huebener P, Taffet G, Entman M, Frangogiannis NG. Interleukin-10 is not a critical regulator of infarct healing and left ventricular remodeling. Cardiovasc Res. 2007; 74:313–322. DOI: 10.1016/j.cardiores.2006.11.028 [PubMed: 17188669]

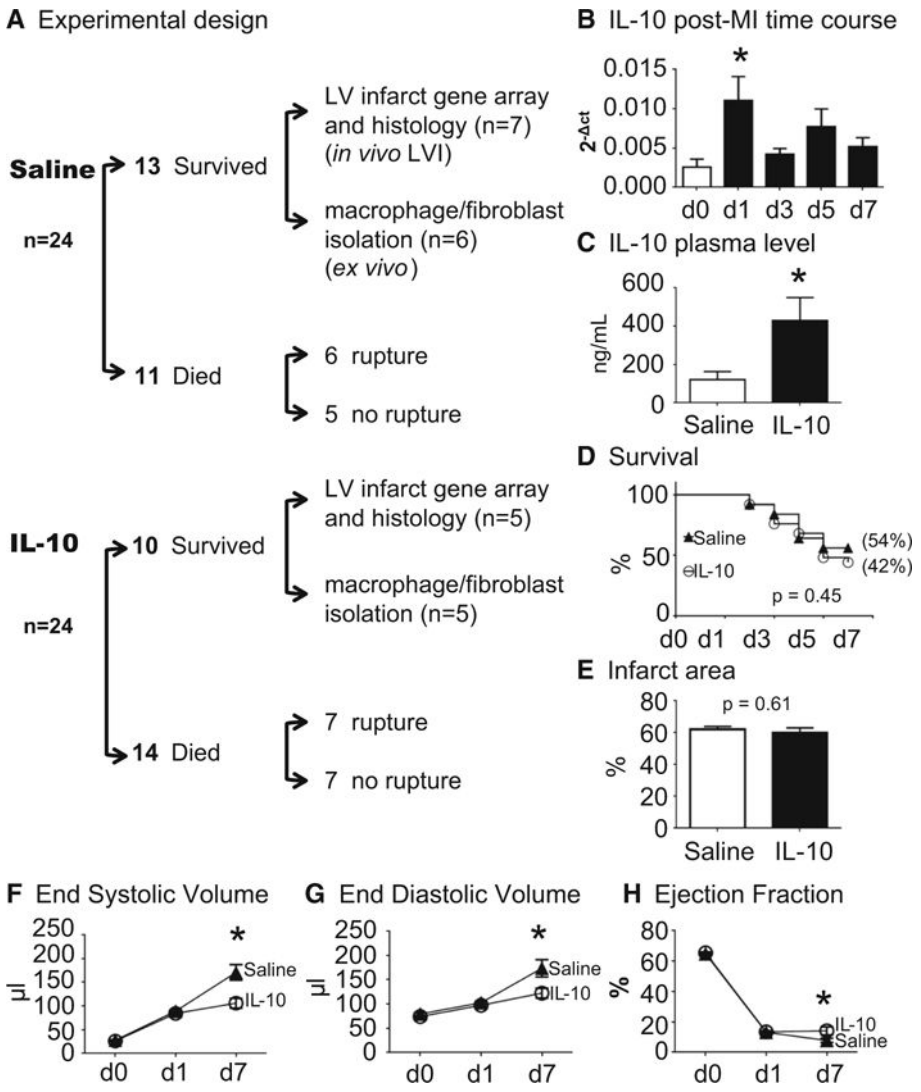

Fig. 1.

IL-10 treatment improved post-MI LV physiology. LV dilation was decreased and ejection fraction increased in the IL-10-treated group at 7 days post-MI.

a Experimental design. **b** IL-10 was elevated in the LV infarct (LVI) at d1 post-MI. **c** IL-10 infusion significantly elevated plasma IL-10 level at 7 days post-MI. IL-10 infusion did not affect d7 post-MI survival rate (**c**) and infarct area (**d**) compared to saline treatment. LV physiology was significantly improved in the IL-10 group compared to saline group. IL-10 treatment resulted in less LV dilation, noted by decreased end-systolic volume (**e**), end-diastolic volume (**f**) and increased ejection fraction (**g**). n = 24/group for survival analysis, n = 10–13/group for physiology measurements,

* $p < 0.05$ vs. saline

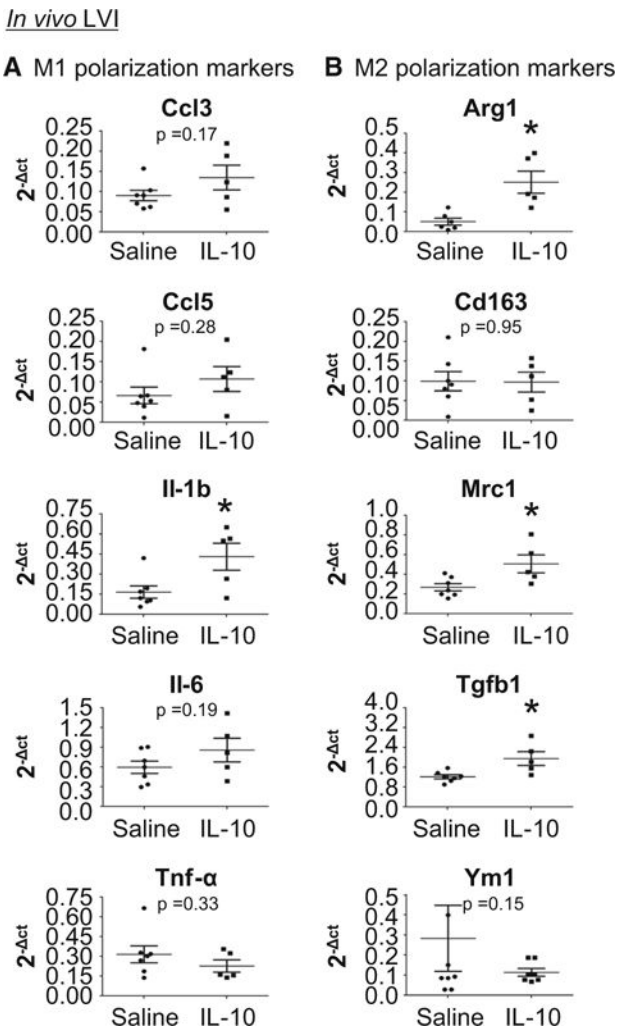

Fig. 2.

IL-10 treatment enhanced the anti-inflammatory response in the LV infarct region (LVI) at d7 post-MI. **a** IL-10 did not affect M1 polarization marker expression. **b** IL-10 elevated anti-inflammatory (M2) marker expression (Arg1, Mrc1, and Tgfb1). $n = 5–7$/group, $*p < 0.05$ vs. saline

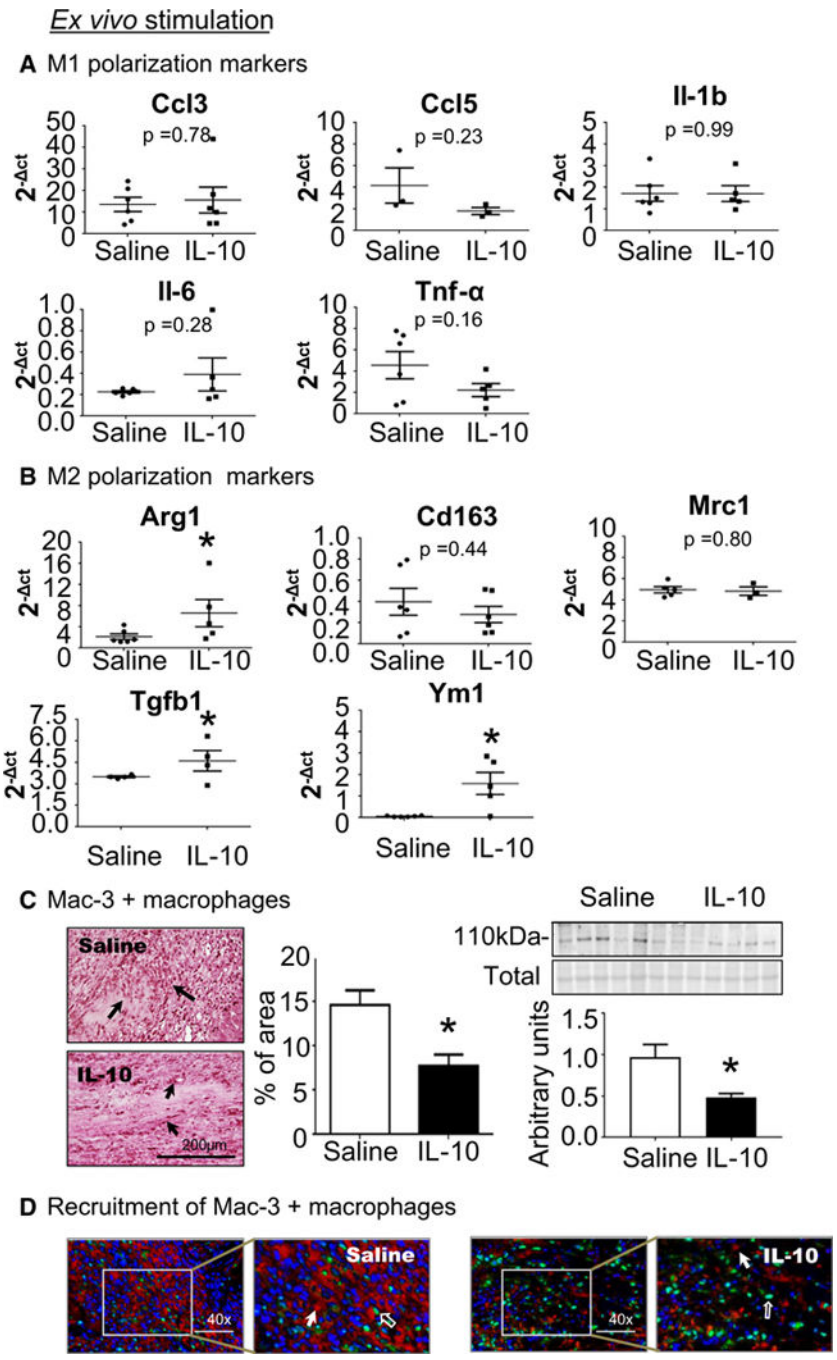

Fig. 3.

IL-10 treatment promoted M2 polarization and decreased cardiac macrophage numbers at 7 days post-MI. Macrophages were isolated from the infarct region at d7 post-MI and evaluated for M1 and M2 markers. **a** IL-10 infusion did not affect expression of M1 markers on ex vivo isolated macrophages. **b** IL-10 treatment stimulated macrophage polarization at d7 post-MI to an M2 phenotype, as isolated macrophages demonstrated elevated expression of Tgfb-1 and Ym1 compared to saline-treated mice. $n = 5–7$/group, $*p < 0.05$ vs. saline. **c** IL-10 treatment decreased macrophage numbers at d7 post-MI. Mac 3 in the LVI was

quantified by immunohistochemistry; arrows indicate positive staining. Sample sizes are five images per section and $n = 5$ sections per group. *$p < 0.05$ vs. saline, scale bar is 200 μm. **d** IL-10 treatment had no effect on macrophage proliferation, as Mac-3 positive cells were not PCNA-positive. Open arrows indicate PCNA (*green*) positive staining, closed arrows indicate Mac-3 (*red*) positive staining and 4′,6-diamidine-2′-phenylindole dihydrochloride (DAPI; *blue*) was used to stain nuclei

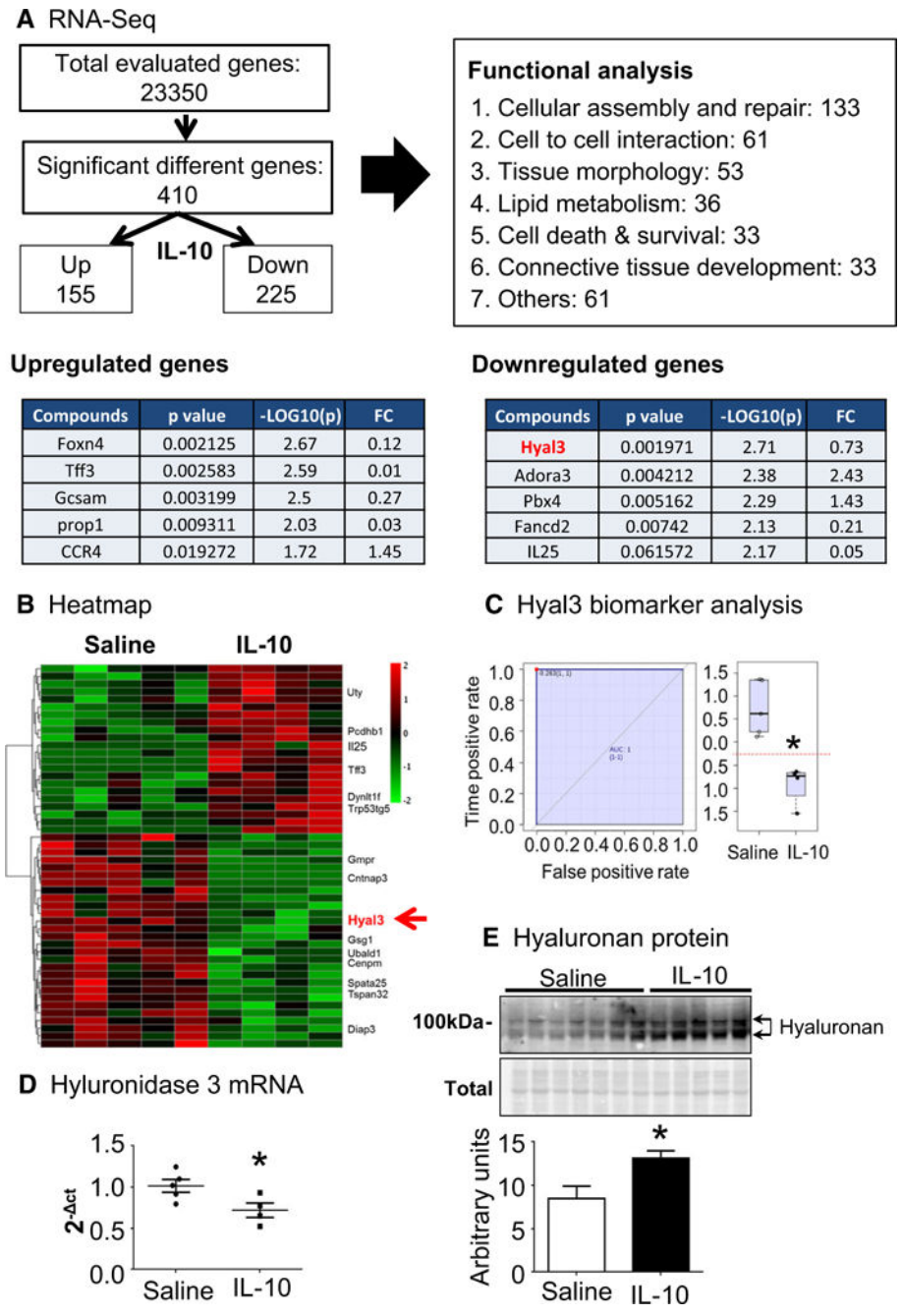

Compounds	p value	-LOG10(p)	FC
Foxn4	0.002125	2.67	0.12
Tff3	0.002583	2.59	0.01
Gcsam	0.003199	2.5	0.27
prop1	0.009311	2.03	0.03
CCR4	0.019272	1.72	1.45

Compounds	p value	-LOG10(p)	FC
Hyal3	0.001971	2.71	0.73
Adora3	0.004212	2.38	2.43
Pbx4	0.005162	2.29	1.43
Fancd2	0.00742	2.13	0.21
IL25	0.061572	2.17	0.05

Fig. 4.

IL-10 decreased hyaluronidase 3 (Hyal3) in cardiac macrophages, which resulted in less turnover of hyaluronic acid (HA). **a** RNA-Seq results and functional group analysis. **b** Heat mapping of the top 50 ranked (by *p* value and fold-change) genes that were differentially expressed in macrophages isolated from the infarcts of IL-10- and saline-treated mice. In the *color legend*, red represents up-regulation of genes compared to saline and *green* represents down-regulation of genes compared to saline. **c** Hyaluronidase 3 (Hyal3) was significantly reduced in LVI macrophages isolated from IL-10-treated mice. **d** RT-PCR results support decreased Hyal3 levels in LVI macrophages isolated from IL-10-treated mice. *n* = 4–5/

group, *$p < 0.05$ vs. saline. **e** By immunoblotting, the IL-10 LVI showed increased full-length hyaluronan acid (HA) due to decreased HA turnover. $n = 5–7$/group, *$p < 0.05$ vs. saline

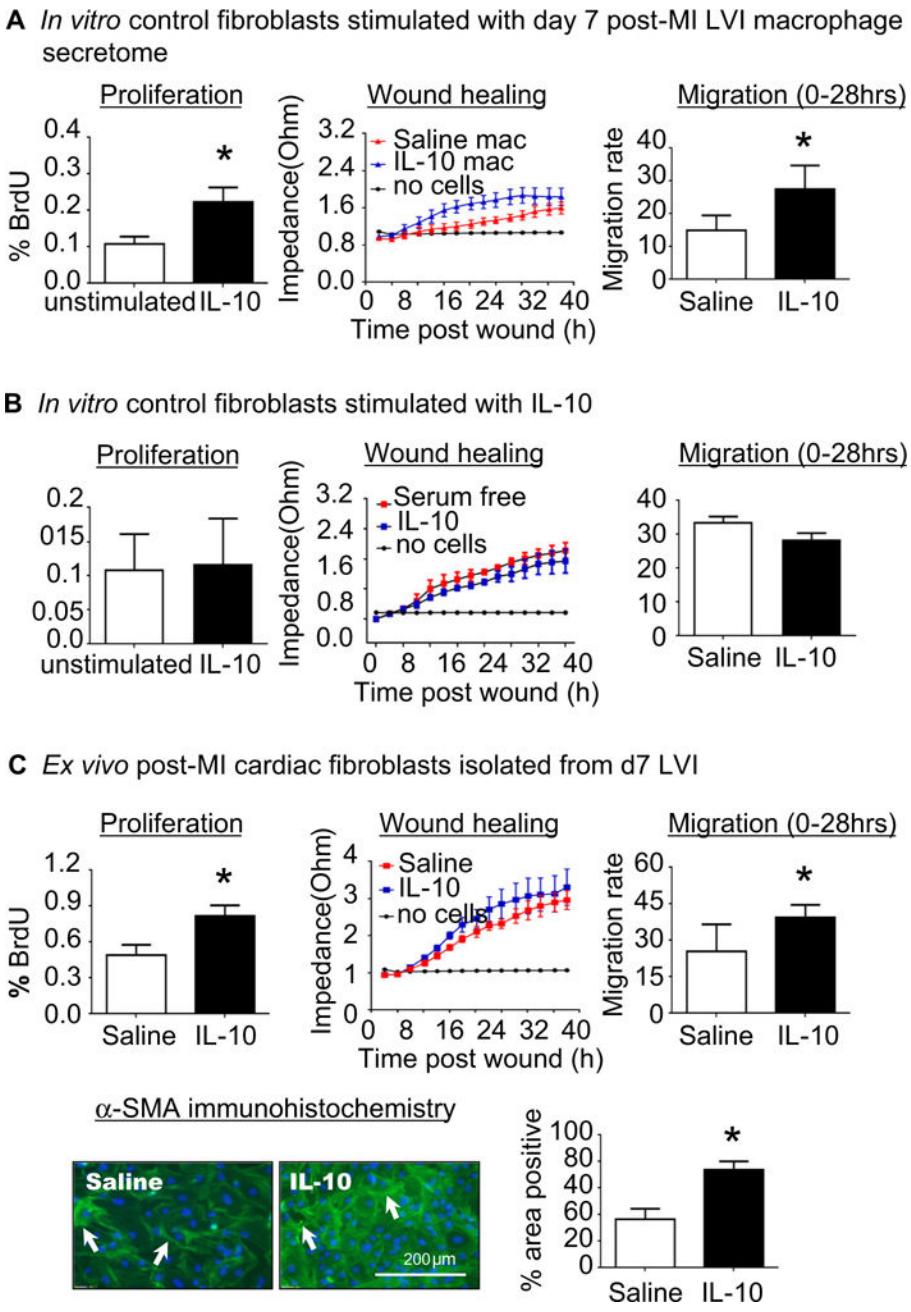

Fig. 5.

IL-10 treatment enhanced post-MI cardiac fibroblast activation and α-SMA expression through indirect effects on macrophage polarization. **a** d0 control cardiac fibroblasts were stimulated with the secretome of macrophages isolated from the d7 LV infarct (LVI) region. The post-MI macrophage secretome from IL-10-treated mice activated fibroblasts, resulting in increased proliferation and migration rates. $n = 4–5$/group, $^*p < 0.05$ vs. saline. **b** Control cardiac fibroblasts stimulated with IL-10 in vitro (50 ng/mL) showed no effect on proliferation or migration rates. $n = 3$/group. **c** Cardiac fibroblasts isolated from d7 LVI showed increased proliferation and migration and α-SMA expression in the IL-10-treated group compared to the saline group. $n = 4–7$/group, $^*p < 0.05$ vs. saline, scale bar is 200 μm

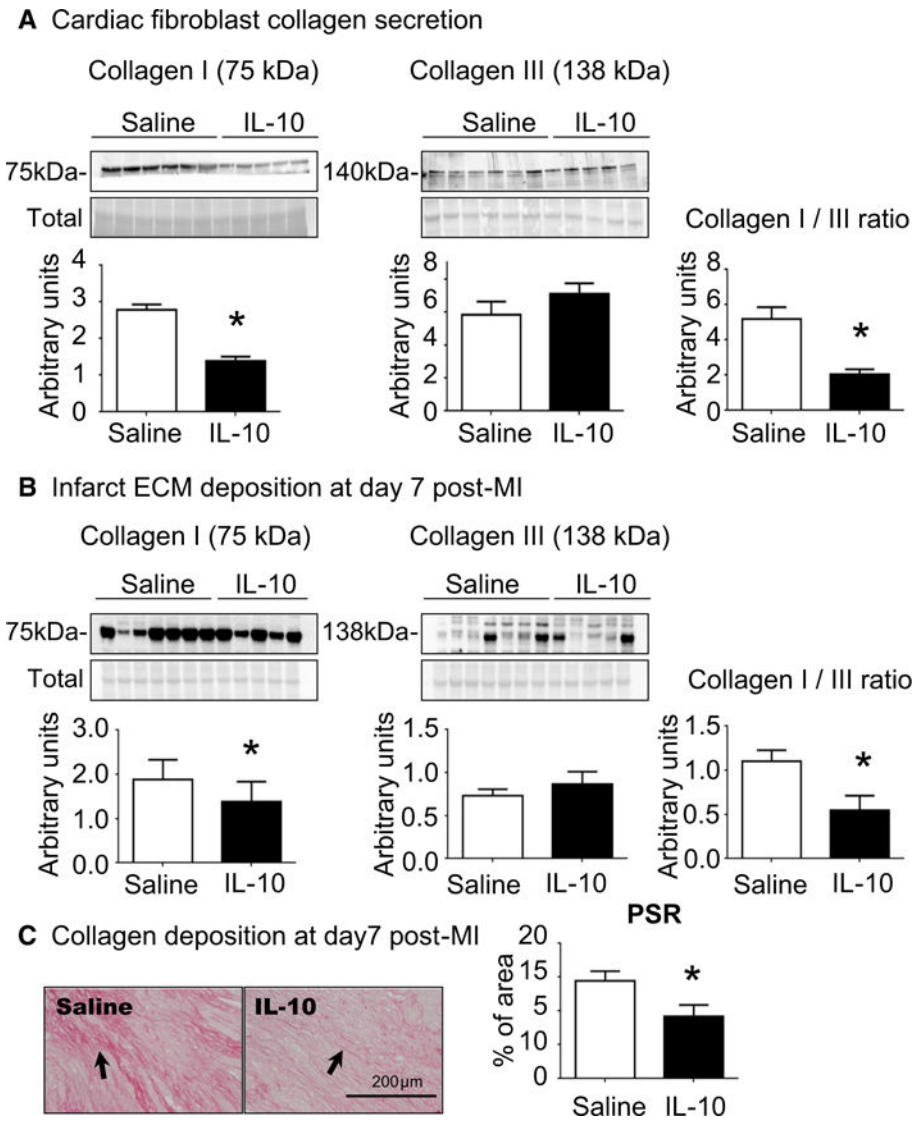

Fig. 6.

IL-10 treatment reduced the ratio of collagen I to collagen III, resulting in decreased fibrosis noted by reduced picrosirius red (PSR) staining. **a** Cardiac fibroblasts isolated from IL-10-treated LVI showed increased collagen I secretion, with no effect on collagen III secretion. The ratio of collagen I to collagen III was significantly reduced by IL-10 treatment. $n = 5–6$/group, $*p < 0.05$ vs. saline. **b** IL-10 treatment significantly decreased the ratio of collagen I to collagen III in the LVI in vivo, consistent with ex vivo findings. For immunoblotting, lanes were normalized by total protein for that lane. $n = 5–7$/group, $*p < 0.05$ vs. saline. **c** Picrosirius red staining showed reduced collagen accumulation in the IL-10-treated LVI at d7 post-MI. Sample sizes are five images for section and $n = 5$ sections per group. $*p < 0.05$ vs. saline, *scale bar* is 200 μm

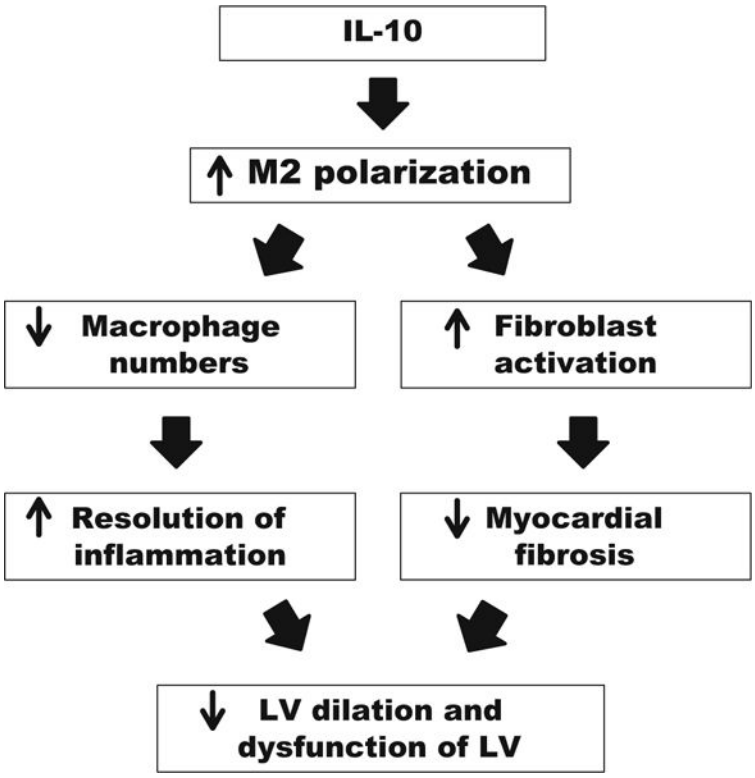

Fig. 7.

Result's summary. IL-10 treatment improved LV physiology by reducing LV dilation post-MI. At d7 post-MI, IL-10 infusion significantly increased M2 polarization of cardiac macrophages, leading to reduced macrophage numbers and cardiac fibroblast activation. This resulted in accelerated inflammation resolution and reduced collagen accumulation. Taken together, our results indicate that the improvement seen with IL-10 treatment was the result of direct actions on macrophage polarization and direct and indirect actions on fibroblast activation